A NOVEL METHOD FOR POLARIMETRIC SAR IMAGE SPECKLE FILTERING AND EDGE DETECTION

PI No. 345

Si-Wei Chen [1], Motoyuki Sato [2]

[1] Graduate School of Environmental Studies, Tohoku University, Japan
[2] Center for Northeast Asian Studies, Tohoku University, Japan
Email: [(1)]chensw@cneas.tohoku.ac.jp, [(2)]sato@cneas.tohoku.ac.jp

ABSTRACT

Speckle filtering and edge detection are fundamental techniques for polarimetric synthetic aperture radar (PolSAR) image analysis. In this paper, based on complex Wishart distribution and the similarity test of the covariance matrix, a completely adaptive speckle filtering is proposed. Meanwhile, a new edge indicator named similar pixel number is developed. This indicator shows great sensitivity to determine the edge pixels and a new edge detection method is proposed. The novelty of this edge detector is that the edge can be detected without mono-edge assumption and the edge orientation can be extracted automatically without any window configurations and searching steps. The efficiency of the proposed speckle filter and edge detection scheme are demonstrated by ALOS/PALSAR data set.

1. INTRODUCTION

Polarimetric SAR (PolSAR) systems have become the mainstream of the microwave remote sensing [1]. Speckle filtering and edge detection are fundamental topics in PolSAR image analysis and interpretation.

As a coherent imaging system, PolSAR is strongly affected by the speckle phenomenon. The existence of speckle will degrade the accuracy of PolSAR image interpretation. The purpose and requirement for the speckle filtering are to select sufficient and the most similar candidate pixels for sample average while preserving the details.

The simplest method is the Boxcar filter which averages the pixels in a local window without any discrimination and inevitably causes a significant blur and dark ring effect. And among the advanced speckle filters proposed in the literature [2], the most relevant ones are the Novak filter [3], the gamma filter [4], the optimal filter [5], and the commonly used Refined Lee filter [6][7]. For the Refined Lee filter, eight edge-aligned windows are defined to locate the most homogeneous area around the considered pixel. The selection of the edge-aligned windows is based on the PolSAR span image. The candidate pixels within the selected window are used to generate an estimator for the covariance matrix based on the linear minimum mean-squared error criteria. In order to avoid the error average of pixels with different polarimetric scattering characters, another model-based algorithm has been developed [8]. This method pays more attention to the scattering mechanism of each pixel, and only the pixels that lie in the same scattering mechanism class will be included for statistical averaging. In addition, an intensity-driven adaptive-neighborhood (IDAN) algorithm has also been introduced [9]. For each seed pixel, a neighborhood with variable shape and dimension, containing only connected pixels, is built by an intensity-driven region growing technique. The main advantage of this method is to gather a significant number of samples without the limitation of the edge-aligned window shape. However, all these methods are not fully adaptive. The selected pixels in Refined Lee method depend on the directional local window. And in IDAN method, the candidate pixels should be connected to each other.

Edge detection is also a fundamental topic for SAR image analysis and has many applications [10]-[14]. Commonly an edge is defined as an abrupt change in image characters between two regions. Due to the speckle phenomenon existing in coherent imaging system, edge detection in SAR images is a difficult task and the differential edge detectors developed for incoherent images are inefficient [15]. For SAR image, several edge detectors adaptive for the special statistics of SAR intensity and complex images are available. Frost et al. [16] proposed one method based on the likelihood ratio (LR) hypothesis tests. Another algorithm based on the normalized ratio of averages (ROA) in the halves of one directional window has also been proposed [15][17]. Optimum edge detection issues including directional window configuration and detection measures are intensively discussed in [18]. To avoid the mono-edge assumption, another optimal multi-edge detector is proposed [19]. Recently, in order to utilize full polarimetric information, a constant false-alarm rate (CFAR) edge detector [20] has also been presented for PolSAR image. This detector is based on the hypothesis statistic test for the Wishart distributed covariance matrix and also adopts the directional window concept. The difference is to test whether the two averaged covariance

matrix on each side of the central pixel are equal and edges are detected when the hypothesis is rejected.

However, these developed edge detectors are always based on the directional window to judge the edge and edge orientation. As pointed out in [21] and [22] , some biased edge location may occur if the edge is not an "ideal" step of known orientation. And if we model and parameterize the window structure, then search the optimal window configuration, as adopted in [18] and [20], it will increase the computation load and the final accuracy is also determined by the window configuration.

In this paper, a new PolSAR image speckle filter and edge detection scheme are proposed. They adopt the complex Wishart distribution statistic test concept which was firstly derived in [23] and also used in [20]. For the speckle filter, we develop a similarity test to select the most similar and sufficient pixels for sample average. Then a new completely adaptive speckle filtering is proposed. For the edge detector, instead of using the traditional directional window, we do the pixels similarity test in a square window and record the number of candidate pixels which are similar to the central pixel. And we found this number is sensitive enough to be a good indicator to judge the edge pixels, since if the central pixel locates at the edge, this number will be much smaller and vice versa for homogeneous case. Besides, the edge orientation can be extracted automatically by moving the square window without any window structure modeling and searching steps.

2. COVARIANCE MATRIX AND SIMILARITY TEST

2.1 Covariance Matrix

For PolSAR, with the reciprocal condition, a three-dimensional scattering vector with linear polarimetric basis can be used

$$k = \begin{bmatrix} s_{hh} & \sqrt{2}s_{hv} & s_{vv} \end{bmatrix}^T \tag{1}$$

where, s_{hv} is the backscattered return from horizontal transmitting and vertical receiving polarization, the other two are similarly defined.

When the imaging area contains many elementary scatterers, k can be modeled as following a multivariate complex Gaussian distribution with mean 0 and covariance matrix C , $k \in N(0, C)$. And the distribution function [1] is

$$p(k) = \frac{1}{\pi^3 |C|} \exp\left(-k^H C^{-1} k\right) \tag{2}$$

where $C = E\left[kk^H \right]$ is the polarimetric covariance matrix, $E(\ldots)$ denotes the expectation value, and $|\quad|$ denotes the determinant .

Commonly, for application, polarimetric covariance matrix is estimated by multi-look processing and the n-look covariance matrix is

$$\hat{C} = \frac{1}{n} \sum_{i=1}^{n} k_i k_i^H \tag{3}$$

where, n is the number of looks and k_i is the i th one look sample.

Let $A = n\hat{C}$, then matrix A follows a complex Wishart distribution $A \in W(q, n, C)$ and the distribution function [1] is

$$p(A) = \frac{|A|^{n-q} \exp\left[-Tr\left(C^{-1} A \right) \right]}{K(n, q) |C|^n} \tag{4}$$

where, $Tr(\cdot)$ denotes the trace of a matrix, and

$$K(n, q) = \pi^{q(q-1)/2} \prod_{j=1}^{q} \Gamma(n - j + 1) \tag{5}$$

The variable q is the dimension of the vector k , $\Gamma(\cdot)$ is the gamma function.

2.2 Similarity Test

Here we set up the binary hypothesis statistic test for examining the similarity of the complex Wishart distributed matrices X and Y , assuming $X \in W(q, n, C_x)$ and $Y \in W(q, n, C_y)$. X and Y have equal multi-look numbers. Then, the null hypothesis is $H_0 : C_x = C_y$ and alternative hypothesis is $H_1 : C_x \neq C_y$.

From [23], the similarity test indicator (likelihood-ratio test statistic) is

$$\ln Q = n\left(2q \ln 2 + \ln|X| + \ln|Y| - 2\ln|X + Y|\right) \tag{6}$$

Assume a constant equivalent multi-look number n for all covariance matrices, (6) can be simplified as

$$\ln Q = \ln|X| + \ln|Y| - 2\ln|X + Y| \tag{7}$$

The proximate probability is

$$P\{-2\rho \ln Q \leq z\} \simeq P\{\chi^2(q^2) \leq z\}$$
$$+ \omega\left[P\{\chi^2(q^2 + 4) \leq z\} - P\{\chi^2(q^2) \leq z\} \right] \tag{8}$$

Where, $\omega = -\dfrac{q^2}{4}\left(1 - \dfrac{1}{\rho}\right)^2 + \dfrac{7}{96}\dfrac{q^2\left(q^2 - 1\right)}{n^2 \rho^2}$ and

$\rho = 1 - \dfrac{2q^2 - 1}{4qn}$.

2.3 Sensitivity Examination

The remained problem is whether the similarity test is sensitive enough to obtain the most similar pixels. Actually, this sensitivity has already been proved by [20], [23]-[25]. Here we will again examine it, shown in Fig. 1. Fig. 1 (a), (c) and (e) show the PolSAR span images (without speckle filtering) with edge pixel, point target pixel and homogenous pixel at the center respectively. Fig. 1 (b), (d) and (f) show the corresponding similarity test results, white colored pixels are labeled as similar to the

(a) (b)

(c) (d)

(e) (f)
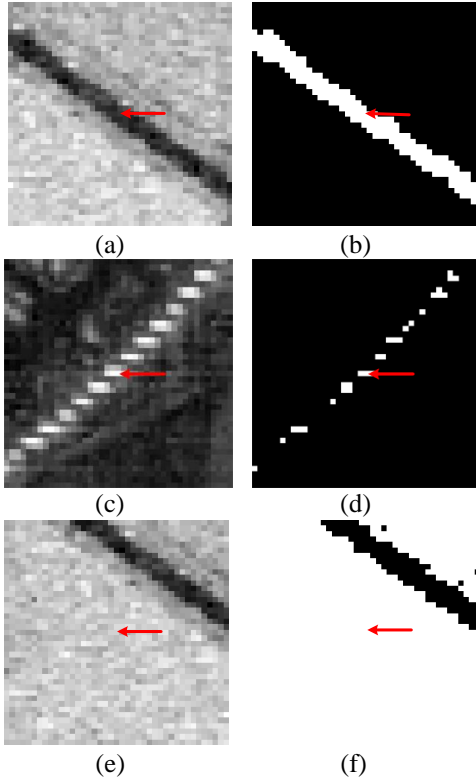
Fig. 1. Similarity test demonstration for the center test pixels (41×41 pixels). (a), (c) and (e) show the PolSAR images with edge pixel, point target pixel and homogenous pixel at the center respectively. (b), (d) and (f) show the similarity test results corresponding to (a), (c) and (e), white colored pixels are judged as candidates which are similar to the center pixel.

center pixel. We can see the results are very accurate according to the terrain characters.

Also note that the proposed similarity test estimation scheme has the ability to collect similar candidates even though they are unconnected. This has the advantage of including sufficient samples which is a basic guarantee for accurate and reliable speckle filtering.

3. SPECKLE FILTERING

Based on the similarity test (SimiTest), a newly developed speckle filtering method [24][25] is proposed, which is dedicated to estimate the polarimetric SAR interferometric(PolInSAR) complex coherence. It is also compatible for PolSAR image speckle filtering and can obtain better performances since it can select the most similar and sufficient pixels for filtering.

The procedure of the SimiTest method is

1) Use the single-look or multi-look complex PolSAR scattering vectors to form the 3×3 C matrix.

2) Then use the 3×3 Boxcar filter to get a rough estimation of the C matrix. Alternatively, in order to avoid any blur and dark ring effect at this early stage, another rough estimation method based on the

similarity parameter [26] between the scattering vectors is adopted. For PolSAR scattering vectors denoted by k_1 and k_2, respectively, the similarity parameter is defined as

$$r(k_1, k_2) = \frac{\left| k_1^H k_2 \right|^2}{\|k_1\|_2^2 \|k_2\|_2^2} \qquad (9)$$

This similarity parameter is calculated pixel by pixel in a local 5×5 edge-aligned window. Then the N ($N = 9$ in this paper) samples with the highest similarity are chosen for the rough estimation. This is equal to a N looks multi-look processing.

3) For each pixel, calculate the similarity test indicators $\ln Q$. The theoretical threshold Th can be obtained from(8). Since there remain some application specifics in the threshold testing, the theoretical threshold needs to be regularly updated according to the data set. One criterion for practical applications is to test some typical edges between two scattering mechanisms and decide the proper thresholds. Then select the most similar pixels according to the intersection of the double similarity test. In order to avoid the case that only very few candidate pixels are chosen, a minimum number $N_{\min}$ of candidates can be predefined.

4) Similarity and distance weighting functions calculation. In order to obtain reliable estimation and enhance the contrast among different terrains, we develop two weighting functions. One is the similarity weighting function

$$\omega_{simi} = \exp\left(-\frac{\ln Q}{\ln Q'}\right) \qquad (10)$$

where, $\ln Q$ and $\ln Q'$ are similarity test values of the selected candidate and the estimated pixel respectively.

Another one is the distance weighting function

$$\omega_d = \exp\left(-r_{ij}\right) \qquad (11)$$

where, r_{ij} is the distance between the candidate and the estimated pixel.
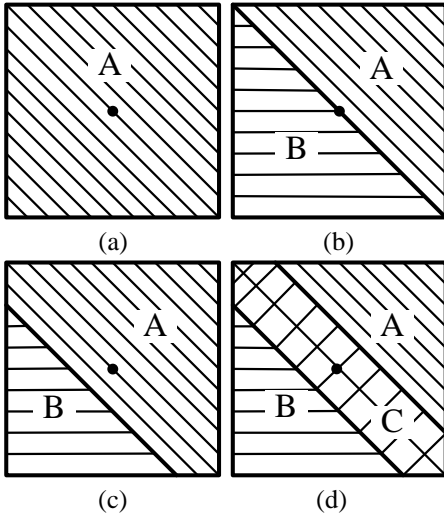
The final weighting function is the combination

$$\omega = \omega_{simi}\omega_d \qquad (12)$$

The physical meaning of this final weighting function is that the more similar and nearer candidate pixels will contribute more to the final estimation results.

5) Finally, PolSAR covariance matrix can be estimated using the candidate pixels

$$\hat{C} = \frac{1}{N}\sum_{i=1}^{N} \omega_i C_i \qquad (13)$$

Fig. 2. Illustration of center pixel category in a small square window. (a) Homogeneous pixel for non-edge case. (b) Edge pixel for mono-edge case. (c) Homogeneous pixel for mono-edge case. (d) Multi-edge case (It can be neglected for small window case).

4. EDGE DETECTION

Since speckle effect will greatly affect the image analysis and the speckle filtering technique is well established, the following discussion is always based on the well speckle filtered PolSAR image.

4.1 Detection Principle

The principle of the proposed edge detection is: do the pixels similarity test in a small square window and record the number of candidate pixels which are similar to the central pixel. The similar pixel number (SPN) is sensitive to be an indicator to determine whether the central pixel is an edge pixel or not, since if the central pixel locates at the image edge, SPN will be much smaller and vice versa for homogeneous case.

As the speckles are well filtered and in order to detect all the micro edges, small $N \times N$ ($N \leq 7$) square window is preferable to test the pixel similarity. Therefore, the properties of pixels in this window can be categorized into mainly four classes (Fig. 2), including homogeneous, mono-edge and multi-edge cases.

1) Homogeneous case (Fig. 2(a)). All pixels in the square window are homogeneous. Ideally the similar pixel number $SPN \approx N^2$.

2) Mono-edge case I (Fig. 2(b)). There are two homogeneous areas in the window labeled A and B. One edge is in the window across the central pixel. Therefore, the similar pixel number $SPN \leq N(N+1)/2$.

3) Mono-edge case II (Fig. 2(c)). There are two homogeneous areas in the window labeled A and B. One edge is also in the window but a bit shifts from

the center. Therefore, the similar pixel number $SPN > N(N+1)/2$.

4) Multi-edge case (Fig. 2(d)). In this case, there are three homogeneous areas in the square window labeled A, B and C. The width of C area is smaller than $(N-1)/2$, otherwise this case should be mono-edge case. Actually, for small window size, this case will not happen and the discussion for SPN is ignored.

Therefore, a conclusion can be obtained from the above analysis: whether the central pixel is edge pixel or not, can be roughly determined by (14)

$$SPN \begin{cases} \leq N(N+1)/2 & Edge\ pixel \\ > N(N+1)/2 & Non-edge\ pixel \end{cases} \qquad (14)$$

4.2 Detection Procedure

Since SPN has the potential to discriminate the edge pixel, a new edge detection scheme can be developed. The procedure of the proposed edge detection method is given in the following

1) PolSAR image speckle filtering.

2) Apply similarity test in a $N \times N$ window. In order to avoid multi-edge case, N should be small enough.

3) Record the SPN based on comparing the similarity indicator (7) with a predefined threshold Th_1, which can be approximately determined by (8) with a given false-alarm probability [23].

4) Normalize the SPN with the window size to scale the value between 0 and 1,

$$SPN = SPN / N^2 \qquad (15)$$

5) Thresholding processing. It is used to obtain the binary rough edge map. Ideally, from (14), this threshold is $Th_2 = (N+1)/(2N)$. Due to the terrain character fluctuation of PolSAR image, commonly Th_2 should be modified a bit larger according to the specific data.

6) Rule out the small noisy edge fragments. This can be done by mathematic morphology based method [27] to delete the fragment smaller than a predefined pixel number.

5. RESULTS

To illustrate the performances of the proposed edge detection method, ALOS/PALSAR full polarimetric SAR data set is used. The test site is mainly seashore terrain in Mayagi, Japan. Fig. 3 shows the investigation area. Fig. 3(a) is the corresponding optical image from Google Map. Fig. 3(b) is the original PolSAR RGB composite image with Pauli scattering components (HH-VV, HV and HH+VV).
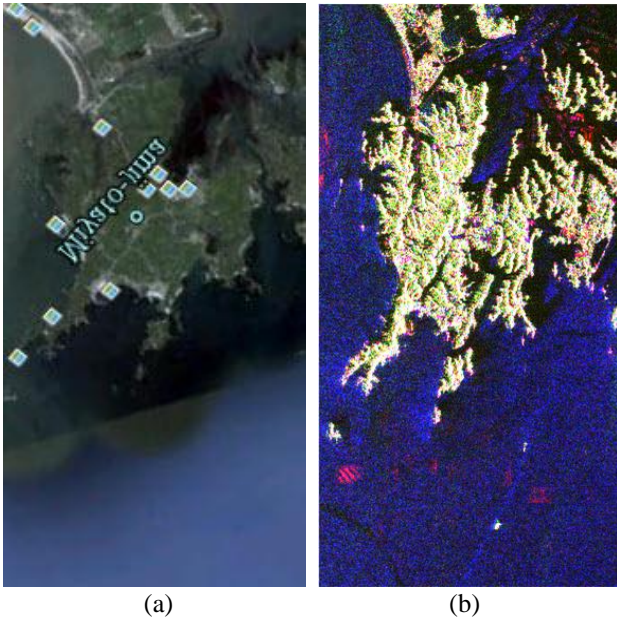
Fig. 3. Optical and the L band ALOS/PALSAR PolSAR images of the test site, Miyagi, Japan (570×300 pixels). (a) Corresponding optical image from Google Map. (b) Original RGB composite image with Pauli scattering components (HH-VV, HV and HH+VV).
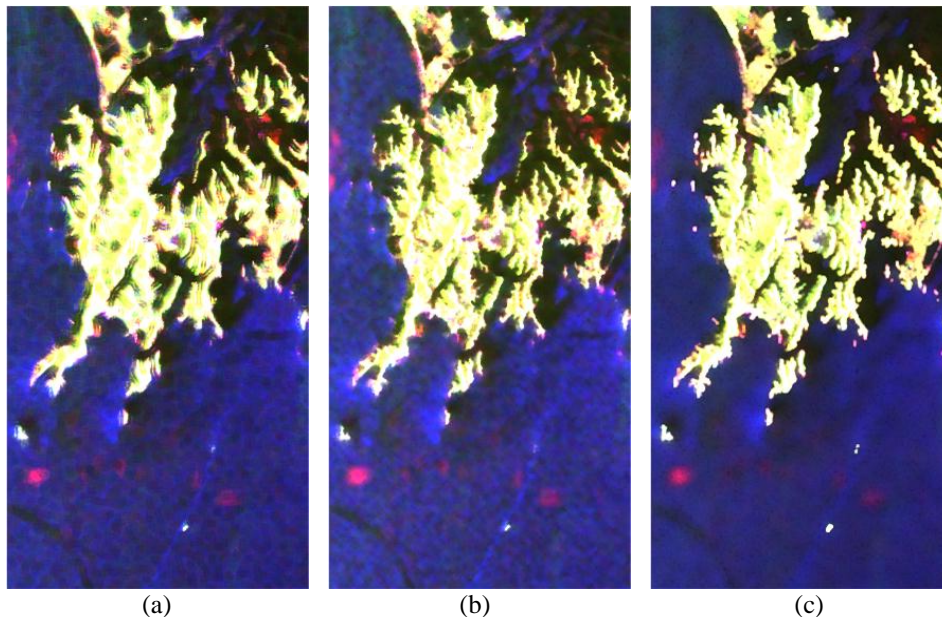
5.1 Speckle filtering

To illustrate the performance of the proposed SimiTest speckle filtering method, the real PolSAR data sets are used. Two speckle filtering algorithms including the Refined Lee and IDAN method are implemented for the comparison purpose. In order to obtain fair comparison, a 9-look multi-look processing is implemented before applying the Refined Lee and IDAN methods. Then for the Refined Lee and IDAN methods, simply but effectively the speckle standard deviation to mean ratio is set to $\sigma_v = 1$. Meanwhile, for the SimiTest speckle filtering method, a 15×15 local square window is used and the minimum number of candidates is $N_{\min} = 10$. The chosen threshold for the SimiTest speckle filtering algorithm is $Th = -4.8$.

Fig .4 shows the speckle filtering results. Compared with the original PolSAR RGB composite images [Fig. 3(b)], the speckles are well smoothed the Refined Lee method [Fig. 4(a)]. However, as mentioned in [9], the fixed size and shape of the edge-aligned windows induce some patchy-look effect all over the image. IDAN method gives much better speckle reduction performance as the details are well preserved. The proposed SimiTest method [Fig. 4(c)] achieves even better speckle reduction and better detail preservation performance, since it can select the sufficient and most similar candidate pixels. Especially, the point targets are well preserved and enhanced. Meanwhile, visually it does not suffer from the patchy-look effect.
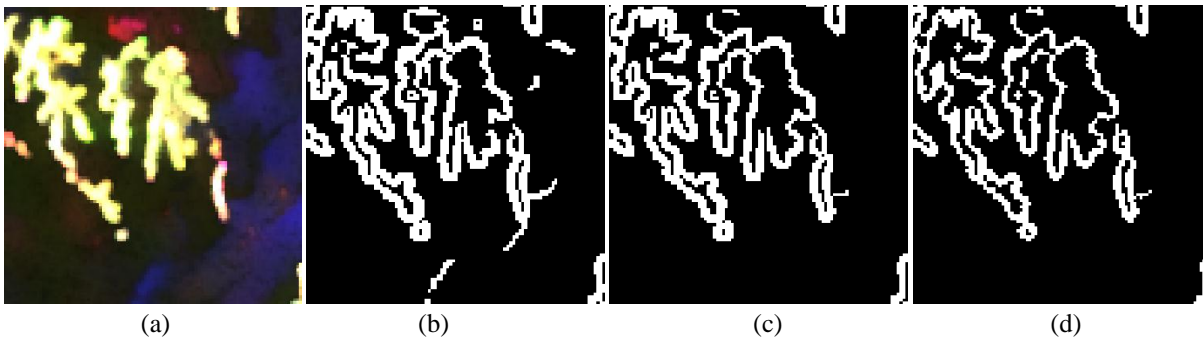
5.2 Edge detection

In order to obtain fair comparison, all the edge detection methods are based on the speckle filtered PolSAR image, processed by the proposed SimiTest method. Also ROA [15] and polarimetric CFAR edge detection [20] methods are implemented for comparison purpose. Four 3×3 local directional windows are used for ROA and polarimetric CFAR edge detection and a 3×3 square window is used for the proposed method. The main edge detection processing includes two steps: first the edge detector is applied to obtain the rough edge map and followed by the post-processing methods to get binary

Fig. 4. Speckle filtered PolSAR images (570×300 pixels). (a) Refined Lee filter, (b) IDAN filter, (c) Proposed method, respectively.
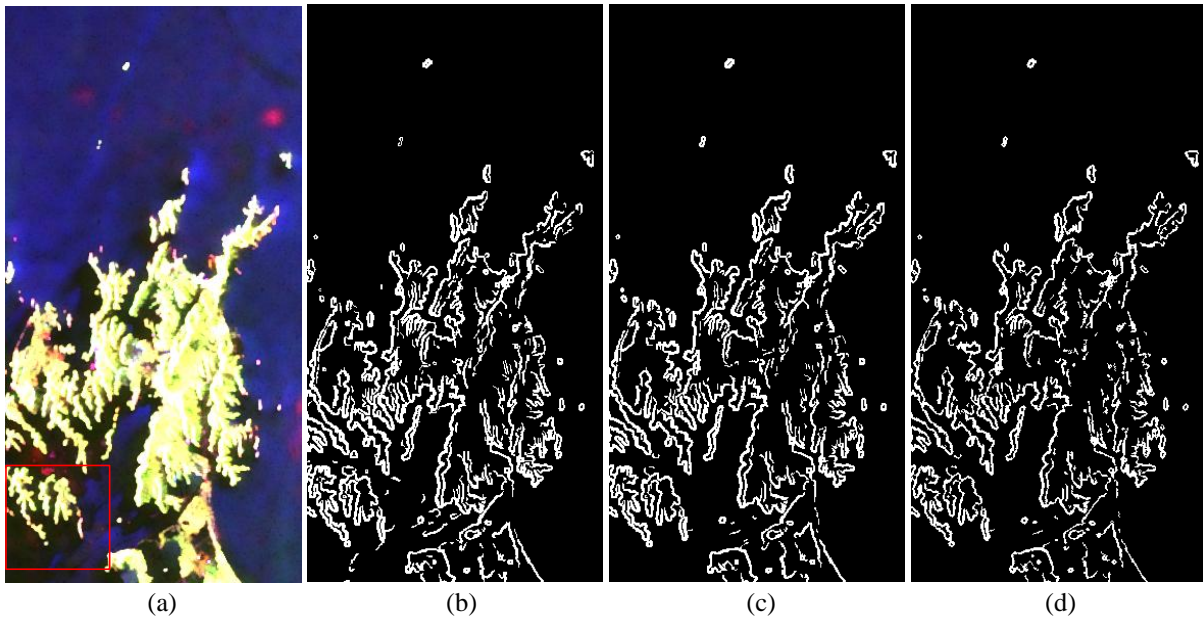
Fig. 5. PolSAR image and final edge detection maps (570×300 pixels). (a) PolSAR RGB composite image with Pauli scattering components (HH-VV, HV and HH+VV), (b)-(c) are final binary edge detection maps by ROA, polarimetric CFAR and the proposed edge detectors respectively.

Fig. 6. Enlarged PolSAR image and final edge detection maps of ROI (100×100 pixels). (a) PolSAR RGB composite image with Pauli scattering components (HH-VV, HV and HH+VV), (b)-(c) are final binary edge detection maps by ROA, polarimetric CFAR and the proposed edge detectors respectively.

edge image and rule out the noisy edges. The thresholds for ROA and polarimetric CFAR detectors are 0.55 and −4.5 respectively. These thresholds can be theoretical calculated from a given false alarm probability and the estimated equivalent number of looks [15][20]. For the proposed edge detector, according to this data set, the two thresholds are $Th_1 = -4.6$ and $Th_2 = 0.67$. Eventually, the noisy edge fragments which are smaller than 5 pixels will be deleted to obtain the final edge map for the three methods.

Fig. 5 and Fig .6 are edge detection results. Fig. 5(a) is the filtered PolSAR RGB composite image with Pauli scattering components. This test site mainly contains ocean, islands and some point targets. Therefore, the edges will be detected at the boundaries among them. Fig. 5(b)-(d) are final edge detection maps after denoising by the ROA, polarimetric CFAR and the proposed edge

detectors respectively. One rectangular region of interest (ROI) in Fig. 5(a) is enlarged for further comparison (see Fig. 6). From the detected edge maps, all the irregular and complicated edges are determined. And on the whole, we can see the detected performances of three edge detectors are almost equivalent. Meanwhile, some differences also can be observed in Fig. 6, that the ROA edge detector shows some false alarms among the shadows while the polarimetric CFAR and the proposed method do not have. It can be interpreted for not utilization of the full polarimetric information by ROA method. In addition, compared with the other two methods, the detected edges by the proposed method are a bit thinner, which is an advantage for further applications.

6. CONCLUSION

The main contributions of this final report lie into two research topics.

Firstly, a new algorithm for PolSAR speckle filtering has been presented. The proposed method is based on the similarity test for complex Wishart distributed covariance matrices. This new method makes full use of the polarimetric information and gives better performance compared to the previous methods. The full usage of information has the ability to select sufficient candidates with the most similar scattering mechanism. A completely adaptive neighborhood with variable shape and dimension according to the similarity test can be formed even without the pixel connection constraint. The experimental results based on real data sets demonstrate the advantage of the proposed method. The speckle effect is greatly reduced while the details are well preserved. Meanwhile, the blur, dark ring and patchy look effects which usually occur in spatial average methods are well avoided. Moreover, this method is almost not affected by the size of the local estimation window, which means a stable and robust estimator can be expected.

Secondly, a new algorithm for PolSAR edge detection has been presented. Based on the similarity test of the covariance matrix, we developed a new indicator named similar pixel number *SPN* for PolSAR image edge detection. The novelty of this edge detector is that the edge indicator *SPN* is obtained in a small square window without edge type assumptions. Besides, the edge orientation can be extracted automatically by moving the square window without any window configurations and searching steps.

The experimental results demonstrate that the proposed edge detection method has almost equivalent performance with the commonly used ROA and polarimetric CFAR edge detectors. Meanwhile, it also benefits for less false alarm edge fragments and a bit thinner detected edges in the final edge map.

Since covariance matrix is equivalent to coherency matrix, the proposed algorithm can be generalized for coherency matrix straightforwardly. Moreover, the proposed method is also compatible for the multi-frequency PolSAR images.

7. ACKNOWLEDGMENTS

8. REFERENCES

[1] J. S. Lee and E. Pottier, *Polarimetric Radar Imaging: From Basics to Applications*, Boca Raton, US: CRC Press, 2009.

[2] R. Touzi, "A review of speckle filtering in the context of estimation theory," *IEEE Trans. Geosci. Remote Sens.*, vol. 40, no. 11, pp. 2392–2404, Nov. 2002.

[3] L. M. Novak and M. C. Burl, Optimal speckle reduction in polarimetric SAR imagery, *IEEE Trans. Aerosp. Electron. Syst.*, 26: 293-305, Mar. 1990.

[4] A. N. Evans, "A gamma filter for multi-look synthetic aperture radar images," *in Proc. ISSPA*, pp. 829–832, 1996.

[5] A. Lopes and F. Sery, Optimal speckle reduction for product model in multilook polarimetric SAR imagery and the wishart distribution, *IEEE Trans. Geosci. Remote Sens.*, 35: 632-647, May 1997.

[6] J. S. Lee, M. R. Grunes, and S. A. Mango, Speckle reduction in multipolarization, multifrequency SAR imagery, *IEEE Trans. Geosci. Remote Sens.*, 29: 535-544, July 1991.

[7] J. S. Lee, M. R. Grunes, and G. de Grandi, "Polarimetric SAR speckle filtering and its implication for classification," *IEEE Trans. Geosci. Remote Sens.*, vol. 37, pp. 2363–2373, Sep. 1999.

[8] J. S. Lee, M. R. Grunes, D. L. Schuler, E. Pottier and L. Ferro-Famil, Scattering-Model-Based Speckle Filtering of Polarimetric SAR Data, *IEEE Trans. Geosci. Remote Sens.*, 44(1): 176-187, Jan. 2006.

[9] G. Vasile, E. Trouve, J. S. Lee, and V. Buzuloiu, "Intensity-driven adaptive-neighborhood technique for polarimetric and interferometric SAR parameters estimation," *IEEE Trans. Geosci. Remote Sens.*, vol. 44, no. 6, pp. 1609–1621, Jun. 2006.

[10] F. Tupin, H.Maitre, J.-F.Mangin, J.-M. Nicolas, and E. Pechersky, "Detection of linear features in SAR images: Application to road network extraction," *IEEE Trans. Geosci. Remote Sens.*, vol. 36, pp. 434–453, Mar. 1998.

[11] F. Tupin, B. Houshmand, and M. Datcu, "Road detection in dense urban areas using SAR imagery and the usefulness of multiple views," *IEEE Trans. Geosci. Remote Sens.*, vol. 40, pp. 2405-2414, Nov 2002.

[12] G. Ferraioli, "Multichannel InSAR Building Edge Detection," *IEEE Trans. Geosci. Remote Sens.*, vol. 48, pp. 1224-1231, Mar 2010.

[13] A. Niedermeier, E. Romaneessen, and S. Lehner, "Detection of coastlines in SAR images using wavelet methods," *IEEE Trans. Geosci. Remote Sens.*, vol. 38, pp. 2270-2281, Sep 2000.

[14] W. G. Zhang, F. Liu, L. C. Jiao, B. A. Hou, S. Wang, and R. H. Shang, "SAR Image Despeckling Using Edge Detection and Feature Clustering in Bandelet Domain," *IEEE Geosci. Remote Sens. Lett.*, vol. 7, pp. 131-135, Jan 2010.

[15] R. Touzi, A. Lopès, and P. Bousquet, "A statistical and geometrical edge detector for SAR images," *IEEE Trans. Geosci. Remote Sens.*, vol. 26, pp. 764–773, Nov. 1988.

[16] V. S. Frost, K. S. Shanmugan, and J. C. Holtzman, "Edge detection for synthetic aperture radar and other noisy images," *IEEE Int. Geosci. Remote Sens. Symp.*, vol. FA2, Munich, Germany, 1982, pp. 4.1–4.9.

[17] A. C. Bovik, "On detecting edges in speckle imagery," *IEEE Trans. Acoust., Speech, Signal Process.*, vol. 36, pp. 1618–1627, Oct. 1988.

[18] C. J. Oliver, D. Blacknell, and R. G. White, "Optimum edge detection in SAR," *Proc. Inst. Elect. Eng.*, vol. 143, no. 1, pp. 31–40, Feb. 1996.

[19] R. Fjørtoft, A. Lopès, P. Marthon, and E. Cubero-Castan, "An optimal multiedge detector for SAR image segmentation," *IEEE Trans. Geosci. Remote Sens.*, vol. 36, pp. 793–802, May 1998.

[20] J. Schou, H. Skriver, A. A. Nielsen, and K. Conradsen, "CFAR edge detector for polarimetric SAR images," *IEEE Trans. Geosci. Remote Sens*, vol. 41, pp. 20-32, Jan 2003.

[21] O. Germain and P. Refregier, "On the bias of the likelihood ratio edge detector for SAR images," *IEEE Trans. Geosci. Remote Sens.*, vol. 38, pp. 1455-1457, May 2000.

[22] O. Germain and P. Refregier, "Edge location in SAR images: Performance of the likelihood ratio filter and accuracy improvement with an active contour approach," *IEEE Trans Image Process.*, vol. 10, pp. 72-78, Jan 2001.

[23] K. Conradsen, A. A. Nielsen, J. Sehou, and H. Skriver, "A test statistic in the complex Wishart distribution and its application to change detection in polarimetric SAR data," *IEEE Trans. Geosci. Remote Sens.*, vol. 41, no. 1, pp. 4-19, Jan. 2003.

[24] S.W. Chen, M. Sato, and X.S. Wang, "PolInSAR Complex Coherence Estimation Based on Covariance Matrix Similarity Test," *IEEE Trans. Geosci. Remote Sens.,2nd Review.*

[25] S.W. Chen, and M. Sato, "PolInSAR Complex Coherence Estimation Based on Similarity Test of Covariance Matrix", *in POLinSAR 2011 Workshop*, Frascati, Italy, Jan. 2011.

[26] J. Yang, Y. N. Peng, and S. M. Lin, "Similarity between two scattering matrices," *Electron. Lett.*, vol. 37, no. 3, pp. 193–194, Feb. 2001.

[27] R.C. Gonzalez, and R.E. Woods, *Digital Image Processing*, Prentice Hall, 2002, ch9, pp.519-549.